Resonances and Aerodynamic Damping of a Vertical Axis Wind Turbine

Fredric Ottermo and Hans Bernhoff

Division for Electricity, Department of Engineering Sciences,
Uppsala University, Box 534, 751 21 Uppsala, Sweden
Email: fredric.ottermo@angstrom.uu.se

May 24, 2012

Abstract

The dynamics of a straight-bladed vertical axis wind turbine is investigated with respect to oscillations due to the elasticity of struts and shaft connecting to the hub. In particular, for the three-bladed turbine, a concept is proposed for dimensioning the turbine to maximize the size of the resonance free rpm range for operation. The effect of aerodynamic damping on the struts is also considered. The damping of these types of oscillations for a typical turbine is found to be good.

1 Introduction

The interest for vertical axis wind turbines (VAWTs) has lately shown a steady increase. One of the reasons for this is their appealing design with few moving parts which could reduce maintenance costs [1], [2]. In comparison to conventional horizontal axis wind turbines, VAWTs have been far less studied, which motivates further research. We consider here a vertical axis, or Darrieus-type [3], turbine with straight blades, also called the H-rotor. This type of turbine has been studied previously in [4] and more recently in for example [5], [6] and [7].

Stability with respect to the per-rev frequencies is a major concern when designing wind turbines. This is normally studied numerically during the design process, see for example [8] for the case of horizontal axis wind turbines and [9] for VAWTs. Torsional eigenmodes of a VAWT due to the elasticity of the drive shaft of a VAWTs was studied in [10]. The approach here is to examine eigenmodes of the H-rotor specifically due to elasticity of struts (in one direction) and shaft below the hub. Compared to most realistic H-rotor designs, a simpler turbine is studied, comprising one horizontal strut

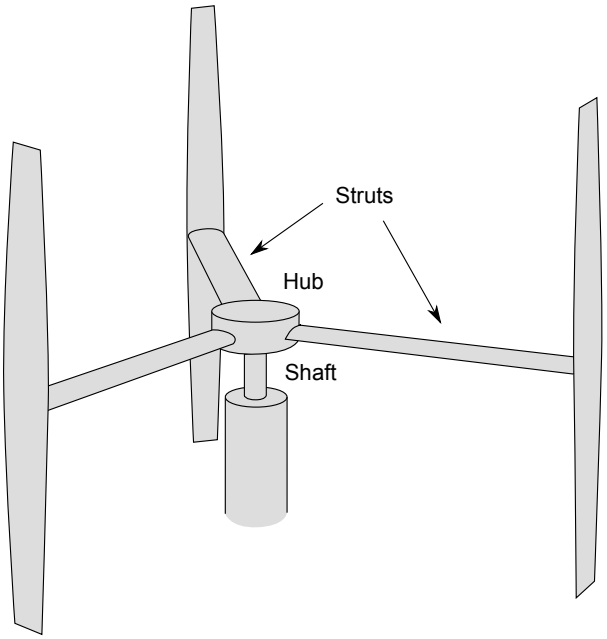

Figure 1: Schematic picture of the three-bladed version of the H-rotor with one horizontal strut per blade.

per blade and point-like mass distribution. This means that many possible eigenmodes of the blade-strut system are not considered by the present analysis. On the other hand, with this approach the eigenmodes can be calculated analytically, which enables a more general study. Furthermore, the overall picture is expected to apply for more realistic turbines as well, in particular the rotational speed dependence. This study shall be viewed as presenting a guideline when designing H-rotors, when it comes to choosing target frequencies to certain eigenmodes. Relating these target frequencies (at least for the parked turbine) to material dimensions for a specific design has to be guided by more exact models, for example by FEM modelling.

An estimation of the aerodynamic damping on the struts is also performed. It is intriguing to see that the damping is good when inserting realistic turbine parameters.

2 H-rotor dynamics

A simple H-rotor design will now be investigated, comprising N blades and N horizontal struts connected to a hub. The three-bladed version of this turbine is shown in Figure 1. The calculation below keeps initially the

number of blades arbitrary, but is later specialized to the case of three blades. The mass of the blade-strut system is considered concentrated to a point at the end of each strut, where the blade connects. The elasticity is modelled by assuming (i) a torque on the hub which is proportional to the deviation angle to the vertical axis, and (ii) the struts being uniform beams with specified stiffness. In what follows we use a cartesian coordinate system such that the z direction is vertical and upwards.

Each strut is modelled as a uniform beam which is primarily elastic in the vertical direction. We define the stiffness k_s of the strut so that the restoring force F at the strut end is $F = -k_\mathrm{s}\Delta z$, where Δz represents the vertical deviation of the strut end with respect to the hub plane. From beam theory, assuming a vertical hub and the strut directed to the x direction, the deflection curve $z(x)$ of the beam is

$$z(x) = -\frac{F}{2k_\mathrm{s}R^3}(3Rx^2 - x^3), \tag{1}$$

where R is the radius of the turbine. In a similar manner the elasticity of the shaft below the hub is taken care of by defining a stiffness k_h so that the restoring torque τ at the hub is $\tau/R = -k_\mathrm{h}\Delta z$, where Δz is here the maximal z deviation at R of an imagined rigid disc attached to the hub.

Let $\boldsymbol{r}_i = (x_i, y_i, z_i)$ be the position of the N point masses, where $i = 1, 2, \ldots, N$ indicate the different masses. With angular velocity Ω of the turbine we may write (for small deflections)

$$x_i = R\cos(\Omega t + 2\pi i/N) \tag{2}$$
$$y_i = R\sin(\Omega t + 2\pi i/N). \tag{3}$$

We want to obtain the vertical positions $z_i(t)$. To start with, the hub direction has to be determined, assuming that $\boldsymbol{r}_i$ are known. Let the hub direction be described by the (dimensionless) vector $\boldsymbol{r}_0 = (x_0, y_0, 1)$, which is tangent to the shaft at the hub. It is possible relate x_0 and y_0 to the point mass positions by requiring that the sum of the torques at the hub be zero. The restoring torque from the shaft is

$$\boldsymbol{\tau}_0 = k_\mathrm{h}R^2(y_0, -x_0, 0), \tag{4}$$

whereas the torques from the struts are given by

$$\boldsymbol{\tau}_i = k_\mathrm{s}\Delta z\ \boldsymbol{r}_i \times \boldsymbol{r}_0. \tag{5}$$

For small deviations we may write $\Delta z = \boldsymbol{r}_i \cdot \boldsymbol{r}_0$, and the torque equation $\boldsymbol{\tau}_0 + \Sigma\boldsymbol{\tau}_i = 0$ may be reduced to

$$y_0(k_\mathrm{h}R^2 + k_\mathrm{s}\Sigma y_i^2) + x_0 k_\mathrm{s}\Sigma x_i y_i + k_\mathrm{s}\Sigma z_i y_i = 0 \tag{6}$$
$$x_0(k_\mathrm{h}R^2 + k_\mathrm{s}\Sigma x_i^2) + y_0 k_\mathrm{s}\Sigma x_i y_i + k_\mathrm{s}\Sigma z_i x_i = 0. \tag{7}$$

Using eqns (2-3) we get for $N \geq 3$

$$x_0 = -\frac{k_\mathrm{s}}{R^2(k_\mathrm{h} + Nk_\mathrm{s}/2)} \Sigma z_i x_i \tag{8}$$

$$y_0 = -\frac{k_\mathrm{s}}{R^2(k_\mathrm{h} + Nk_\mathrm{s}/2)} \Sigma z_i y_i. \tag{9}$$

(A special treatment is needed for $N = 2$, the result is indicated in connection to eqn (14) below.) Once the hub orientation is determined it is possible to write down the vertical forces F_i acting on the point masses. The total vertical force is

$$F_i = F_{\mathrm{s},i} + F_{\mathrm{c},i} + F_{\mathrm{d},i}, \tag{10}$$

where $F_{\mathrm{s},i}$ is the restoring force from strut deflection, $F_{\mathrm{c},i}$ is the vertical component of the centripetal force, and $F_{\mathrm{d},i}$ is the aerodynamic damping force. We start by determining the eigenmodes while ignoring the damping term. From the definition of k_s we know that

$$F_{\mathrm{s},i} = -k_\mathrm{s}\ \boldsymbol{r}_i \cdot \boldsymbol{r}_0. \tag{11}$$

For small deflections the centripetal force is $mR\Omega^2$, where m is the mass of the point masses. Apart from the restoring force due to deflection, the remaining force from the strut will be tangent to the strut and have magnitude $mR\Omega^2$. We find, using eqn (1), that the slope of the strut end is $(\frac{3}{2}\Delta z + \Delta\tilde{z})/R$, where Δz is the part of the deviation that corresponds to strut deflection and $\Delta\tilde{z}$ the part due to hub mis-alignment. Using the fact that $\Delta z + \Delta\tilde{z} = z$, the vertical component can be written

$$F_{\mathrm{c},i} = -\left(\frac{1}{2}\boldsymbol{r}_i \cdot \boldsymbol{r}_0 + z_i\right) m\Omega^2 \tag{12}$$

The dynamics is obtained by letting $m\ddot{z}_i = F_i$. We then have

$$\ddot{z}_i = -\frac{k_\mathrm{s}}{m}\ \boldsymbol{r}_i \cdot \boldsymbol{r}_0 - \Omega^2\left(\frac{1}{2}\boldsymbol{r}_i \cdot \boldsymbol{r}_0 + z_i\right) \tag{13}$$

which simplifies to the following system of equations,

$$\begin{bmatrix} \ddot{z}_1 \\ \vdots \\ \ddot{z}_N \end{bmatrix} = \begin{bmatrix} A - B & \cdots & A\cos\delta_{1N} \\ \vdots & \ddots & \vdots \\ A\cos\delta_{N1} & \cdots & A - B \end{bmatrix} \begin{bmatrix} z_1 \\ \vdots \\ z_N \end{bmatrix}, \tag{14}$$

where

$$A = \frac{k_\mathrm{s}/m + \Omega^2/2}{k_\mathrm{h}/k_\mathrm{s} + N/2}, \tag{15}$$

$$B = \frac{k_\mathrm{s}}{m} + \frac{3}{2}\Omega^2, \tag{16}$$

and the off-diagonal elements are $A\cos\delta_{ij}$ where $\delta_{ij} = 2\pi(i-j)/N$ with i and j indicating rows and columns. Eqn (14) is valid also for $N = 2$ if $N/2$ is replaced by N in eqn (15). The general solution to eqn (14) is a superposition of harmonic oscillations with frequencies $\omega_i = \sqrt{-\lambda_i}$, where λ_i are the eigenvaules of the matrix in eqn (14). (As expected for physical reasons, all eigenvalues are negative.)

2.1 Modes of the three-bladed turbine

The most common number of blades for large H-rotors is two or three. In what follows we will focus on the case of three blades and examine the corresponding modes, which may be relevant for the recent 200 kW H-rotor design studied in [11]. For $N = 3$ we get the frequencies $\omega_1 = \sqrt{B}$ and $\omega_2 = \omega_3 = \sqrt{B - 3A/2}$. Defining $\tilde{\omega}_1$ and $\tilde{\omega}_2$ as the frequencies for parked turbine $\Omega = 0$, we may rewrite the frequencies more conveniently as

$$\omega_1 = \tilde{\omega}_1\sqrt{1 + \frac{3\Omega^2}{2\tilde{\omega}_1^2}} \tag{17}$$

and

$$\omega_2 = \omega_3 = \tilde{\omega}_2\sqrt{1 + \frac{\Omega^2}{2\tilde{\omega}_1^2} + \frac{\Omega^2}{\tilde{\omega}_2^2}}, \tag{18}$$

where

$$\tilde{\omega}_1 = \sqrt{\frac{k_\mathrm{s}}{m}} \qquad \text{and} \qquad \tilde{\omega}_2 = \sqrt{\frac{k_\mathrm{h}}{m}\left(\frac{k_\mathrm{h}}{k_\mathrm{s}} + \frac{3}{2}\right)^{-1}}. \tag{19}$$

We note that $0 < \tilde{\omega}_2 < \tilde{\omega}_1$. The corresponding solutions are

$$z_{i,(1)} = a_1 \sin\omega_1 t \tag{20}$$

and

$$z_{i,(2,3)} = a_2 \sin\left(\omega_2 t \pm i\frac{2\pi}{3}\right), \tag{21}$$

where a_1 and a_2 are constants.

Let us examine these solutions in some detail. The first solution $z_{i,(1)}$ corresponds to all masses oscillating in phase. (As expected, this frequency is independent of the hub stiffness $k_\mathbf{h}$.) This mode will primarily couple to the third per-rev frequency 3P (and multiplications, i.e. 6P, 9P etc.). The second and third solutions are somewhat more involved since the phase differs between the masses. For these modes to strongly couple to a per-rev frequency we need the phase of $z_{1,(2,3)}(t)$ to equal the phase of $z_{2,(2,3)}(t + 2\pi/3\Omega)$. Hence, for coupling we need

$$\omega_2 t + M2\pi = \omega_2\left(t + \frac{2\pi}{3\Omega}\right) \pm \frac{2\pi}{3}, \tag{22}$$

where M is an integer. This implies that $\omega_2 = (3M \pm 1)\Omega$, and the modes will couple to every per-rev frequency except 3P, 6P and so on. However, we note that $\omega_2 > \Omega$ for all Ω, so coupling to 1P is not possible. Therefore the strongest coupling is expected to occur for 2P and 4P.

To get optimal efficiency one typically wants to keep the tip speed ratio constant, which implies a variable rotational speed. It is then desirable to have an as large resonance free rpm range as possible. One obvious possibility is to make the turbine stiff enough to keep ω_1 and ω_2 well above the lowest per-rev frequencies. However, for large turbines this might not be a realistic option considering the extreme dimensions required for the shaft. To account for this we propose to dimension the turbine so that the 2P resonance of ω_2 and the 3P resonance of ω_1 coincides. Then we get a resonance free region between the 6P and 3P resonances of ω_1. With this choice $\tilde{\omega}_2 = \sqrt{3/8}\ \tilde{\omega}_1$ and the resonance free range becomes $0.17\ \tilde{\omega}_1 < \Omega < 0.36\ \tilde{\omega}_1$. Figure 2 exemplifies this by a Campbell diagram.

The Ω dependence seen in Figure 2 is reasonable for these types of oscillations influenced by a centrifugal force. We may compare to the modes examined in [9], where a curved-bladed full-Darrieus turbine is studied. These modes are generally quite different from the ones studied here due to the difference in geometry, but for example mode 10 is expected to experience similar forces and the Ω dependence is indeed similar.

The model presented here is not intended to be used to calculate the parked frequencies $\tilde{\omega}_1$ and $\tilde{\omega}_2$ of real H-rotor designs, which typically have more complicated struts and mass distributions. Instead, $\tilde{\omega}_1$ and $\tilde{\omega}_2$ need to be determined by models that take the exact geometry into account, for example by means of FEM modelling. Using such methods for the parked frequencies, it is expected that the present analysis correctly reflects the main characteristics of the corresponding modes and in particular the Ω dependence. The results presented here may then be used in the following way in the design process of an H-rotor. Assuming that a desired rpm range of the turbine is at hand, the proposed design process starts with adjusting the stiffness of the struts so that the parked frequency $\tilde{\omega}_1$ equals $\Omega/0.36$ where Ω is upper limit of the rpm range plus some safety margin. Then the stiffness of the hub shaft is adjusted so that $\tilde{\omega}_2 = \sqrt{3/8}\ \tilde{\omega}_1$. As said before, in this process accurate models (FEM) should be used to relate the frequencies $\tilde{\omega}_1$ and $\tilde{\omega}_2$ to material dimensions.

2.2 Aerodynamic damping

The damping effect due to the aerodynamic force on the struts will now be estimated. H-rotors are generally designed so that the strut beams are more or less airfoil-shaped to minimize drag. It is therefore possible to model the aerodynamic force by simply assuming a lift proportional to the angle of attack, since this will be small. (This holds for the horizontal struts

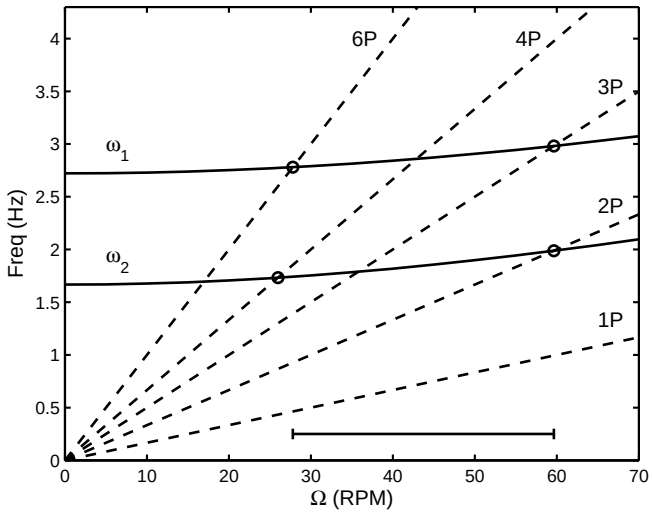

Figure 2: Example of a Campbell diagram for the simplified three-bladed H-rotor, with the proposed dimensioning of the turbine. The parked frequency $\tilde{\omega}_2 = \omega_2(0)$ is here chosen to be 100 rpm. The resonance free rpm range is indicated in the plot (ranges from 28 rpm to 59 rpm).

considered here. For tilted struts, the angle of attack may reach the stall region for low tip speed ratios, in which case the estimate presented here do not apply). In a similar manner there will be aerodynamic damping on the blades for these oscillations, a contribution which is not included in this estimate. The calculation presented here serves as an order of magnitude estimate, and the real damping will be further enhanced by the blades.

Write the lift coefficient as $C_L = c\alpha$, where α is the angle of attack and c is a constant chosen to be 4 rad^{-1}, which is a conservative choice. We assume for simplicity a constant background wind distribution $\boldsymbol{V} = V\hat{\boldsymbol{x}}$ that is unperturbed by the turbine. The relative wind speed $\boldsymbol{v}_i$ at a point $\boldsymbol{r} = \eta\boldsymbol{r}_i$ along the strut is $\boldsymbol{v}_i = \boldsymbol{V} - \eta\dot{\boldsymbol{r}}_i$. However, it is only the speed component $\tilde{v}_i$ perpendicular to the strut that generates lift. We may write $\tilde{v}_i = \boldsymbol{v}_i \cdot \dot{\boldsymbol{r}}/|\dot{\boldsymbol{r}}|$, so that

$$\tilde{v}_i = \frac{V\dot{x}_i}{R\Omega} - \eta R\Omega = -R\Omega\left(\frac{y_i}{\nu R} + \eta\right), \tag{23}$$

where ν is the tip speed ratio. The aerodynamic damping force can now be written as

$$F_{\mathrm{d},i} = \frac{1}{2}\rho w \int C_L \tilde{v}_i^2 \eta R d\eta, \tag{24}$$

where ρ is the density of air, w is the width of the strut and the integral is taken at least over the airfoil part of the strut. The extra η in the integrand takes care of difference in lever arms between the lift position and the point mass position. The angle of attack as a function of η will differ between the modes. For the first mode (ω_1) we get from eqn (1) the vertical speed at $\boldsymbol{r} = \eta\boldsymbol{r}_i$ to be $\frac{1}{2}(3\eta^2 - \eta^3)\dot{z}_i$, whereas for the other modes (ω_2) it is closer to $\eta\dot{z}_i$ since the struts are not as bent. At realistic tip speed ratios (around 4) the dominant contribution is the second term of eqn (23), while the first is term is just a small variation of the damping during the revolution, with small net contribution. Therefore, we exclude the first term of eqn (23), and the main damping may be considered due to the force

$$F_{\mathrm{d},i} = \frac{1}{2}\rho w c R^2 \Omega \xi \ \dot{z}_i \tag{25}$$

where we have integrated along the whole strut ($0 < \eta < 1$). ξ is between 0.19 and 0.25 depending on the mode, the lower value corresponding to the first mode, which is somewhat less damped. (The blade damping will however be stronger for this mode.) It is convenient to express the amount of damping through the damping ratio ζ, which here becomes $\zeta = F_{\mathrm{d},i}/(2m\omega\dot{z}_i)$. For realistic dimensions, say $w = 1$ m, $R = 10$ m and $m = 200$ kg (these data relate to the recent 200 kW H-rotor design studied in [11]), we get for the first mode at the 3P resonance a damping ratio of $\zeta = 0.04$, and for the other modes at the 2P resonance we get $\zeta = 0.08$. This might appear as small numbers (far from critical damping $\zeta = 1$), but

$\zeta = 0.04$ at 3P corresponds to a reduction of the amplitude of about 50% per turbine revolution, and $\zeta = 0.08$ at 2P corresponds to a reduction of about 60%, which is substantial. Looking at the amplitude reduction per turbine revolution, the numbers are identical also for the 6P and 4P resonances. We emphasize that one should operate in the resonance free rpm range, but it is intriguing to see that the damping is good for realistic turbine parameters. Note that the damping is proportional to the width of the struts, so from this point of view the struts should be given a wide design. There is however a trade-off since the construction will then be more sensitive to vertical wind speed components.

3 Conclusion

Oscillations of a simple H-rotor due to the elasticity of struts and shaft connecting to the hub have been investigated. The eigenmodes of the three-bladed turbine have been calculated and examined with respect to coupling to the per-rev frequencies. It was found that it is possible to obtain a large resonance free rpm range by a careful dimensioning of the turbine. Also, if the struts are wide and airfoil-shaped, the aerodynamic damping of these eigenmodes was found to be good. It would be interesting to compare the results with experiments on for example the 200 kW H-rotor studied in [11].

Acknowledgements

This work was conducted within the STandUP for ENERGY strategic research framework. The Swedish Energy Agency, VINNOVA and Statkraft are acknowledged for supporting the Swedish Centre for Renewable Electric Energy Conversion.

References

[1] S. Eriksson, H. Bernhoff, and M. Leijon. Evaluation of different turbine concepts for wind power. *Renewable and Sustainable Energy Reviews*, 12(5):1419 – 1434, 2008.

[2] S. Peace. Another approach to wind. *Mechanical Engineering*, 126(6):28, 2004.

[3] G.J.M. Darrieus. Turbine having its rotating shaft transverse to the flow of the current. us patent 1.835.018. December 1931.

[4] C.A. Morgan, P. Gardner, I.D. Mays, and M.B. Anderson. The demonstration of a stall regulated 100 kw vertical axis wind turbine. *Proc. 1989 European Wind Energy Conference, Glasgow, Scottland*, 1989.

[5] C. J. Simo Ferreira, A. Van Zuijlen, H. Bijl, G. Van Bussel, and G. Van Kuik. Simulating dynamic stall in a two-dimensional vertical-axis wind turbine: Verification and validation with particle image velocimetry data. *Wind Energy*, 13(1):1–17, 2010.

[6] N. Qin, R. Howell, N. Durrani, K. Hamada, and T. Smith. Unsteady flow simulation and dynamic stall behaviour of vertical axis wind turbine blades. *Wind Engineering*, 35(4):511–527, 2011.

[7] J. Kjellin, F. Blow, S. Eriksson, P. Deglaire, M. Leijon, and H. Bernhoff. Power coefficient measurement on a 12 kw straight bladed vertical axis wind turbine. *Renewable Energy*, 36(11):3050–3053, 2011.

[8] T.L. Sullivan. A review of resonance response in large, horizontal-axis wind turbines. *Solar Energy*, 29(5):377 383, 1982.

[9] T. G. Carne, D. W. Lobitz, A. R. Nord, and R. A. Watson. Finite element analysis and modal testing of a rotating wind turbine. *Report No. SAND82-0345, Albuquerque, New Mexico: Sandia National Laboratories*, 1982.

[10] S. Eriksson and H. Bernhoff. Generator-damped torsional vibrations of a vertical axis wind turbine. *Wind Engineering*, 29, 2005.

[11] S. Eriksson, H. Bernhoff, and M. Leijon. A 225kw direct driven pm generator adapted to a vertical axis wind turbine. *Advances in Power Electronics*, 2011, 2011.